Energy Conversion and Management 89 (2015) 458–472

Contents lists available at ScienceDirect

Energy Conversion and Management

journal homepage: www.elsevier.com/locate/enconman

Evaluating the value of batteries in microgrid electricity systems using an improved Energy Systems Model

Eric Hittinger [a,*], Ted Wiley [b], John Kluza [b], Jay Whitacre [b,c,d]

[a] Department of Public Policy, Rochester Institute of Technology, Rochester, NY 14623, United States
[b] Aquion Energy, 32 39th Street, Pittsburgh, PA 15201, United States
[c] Department of Materials Science and Engineering, Carnegie Mellon University, Pittsburgh, PA 15213, United States
[d] Department of Engineering and Public Policy, Carnegie Mellon University, Pittsburgh, PA 15213, United States

ARTICLE INFO

Article history:
Received 25 April 2014
Accepted 6 October 2014
Available online 24 October 2014

Keywords:
Microgrid
Battery
Lead-acid
Aqueous Hybrid Ion
Economics
System modeling

ABSTRACT

A high-resolution model allowing for the comparison of different energy storage technologies in a variety of realistic microgrid settings has been developed. The Energy Systems Model (ESM) is similar to the popular microgrid software HOMER, but improves upon the battery models used in that program. ESM adds several important aspects of battery modeling, including temperature effects, rate-based variable efficiency, and operational modeling of capacity fade and we demonstrate that addition of these factors can significantly alter optimal system design, levelized cost of electricity (LCOE), and other factors. ESM is then used to compare the Aqueous Hybrid Ion (AHI) battery chemistry to lead acid (PbA) batteries in standalone microgrids. The model suggests that AHI-based diesel generator/photovoltaic (PV)/battery systems are often more cost-effective than PbA-based systems by an average of around 10%, even though the capital cost of AHI technology is higher. The difference in LCOE is greatest in scenarios that have lower discount rates, increased PV utilization, higher temperature, and more expensive diesel fuel. AHI appears to be a better complement to solar PV, and scenarios that favor the use of solar PV (low PV prices, low discount rates, and high diesel prices) tend to improve the LCOE advantage of AHI. However, scenarios that do not require constant cycling of the batteries strongly favor PbA. AHI is not a drop-in replacement for PbA. To minimize LCOE, microgrids using AHI batteries should be designed and operated differently than PbA microgrids.

1. Background

Microgrids are small self-reliant electricity grids that produce and distribute power across a limited area, such as a village or industrial complex. Microgrids can be grid-tied, where the system is able to connect with a larger traditional grid, or standalone systems where there is no outside electrical connection. The Energy Systems Model and this paper focus only on standalone systems.

Standalone microgrids have traditionally been a very niche market, appropriate only for applications where less expensive traditional grids could not operate [1,2]. But continual improvements in the performance and cost of microgrid technologies (ex. PV, small wind, and batteries) are making microgrids a more attractive option, particularly in developing or remote areas that have not yet invested in traditional grid infrastructure [1,3]. Microgrids have several advantages over traditional grids: they are scalable and do not require large capital investment, they are generally environmentally superior to traditional generation, and they can be tailored to the particular needs of a community [4–6]. But cost is always an important factor, and any serious discussion of microgrid technology must effectively address that issue.

Evaluating microgrid systems involves significant complexity and uncertainty. This complexity and uncertainty relates to both the design of the microgrid system (such as the scale of different energy sources and quantity of storage to purchase and install) and to the operation of an existing system (such as dispatch algorithms for storage and generation) [2]. Furthermore, the design and operation are somewhat interdependent: the optimal design depends on the way that the system will be operated and the optimal operation depends on the system design. This optimization is made more complex by uncertainty in actual load and renewable resource as well as price uncertainty for variable costs such as diesel fuel. Fortunately, the objective in microgrid design is normally very simple: to meet load with the lowest levelized cost

* Corresponding author. Tel.: +1 585 475 5312; fax: +1 585 475 2510.
E-mail addresses: eshgpt@rit.edu (E. Hittinger), twiley@aquion-energy.com (T. Wiley), whitacre@andrew.cmu.edu (J. Whitacre).

http://dx.doi.org/10.1016/j.enconman.2014.10.011
0196-8904/

of electricity (LCOE) or lowest net present cost (NPC) through the expected lifetime of the system. However, even this is complicated by questions of reliability: a lower LCOE can be attained if you are tolerant of more frequent power outages. For all of these reasons, one cannot expect to achieve the perfectly optimal microgrid system design or operation. Rather, several simplifying assumptions must be made and an acceptable compromise chosen from a more constrained set of options.

Due to both the growing importance of microgrids and the complexity of microgrid optimization, a significant quantity of academic research has been produced about microgrid operation, design, and economics. A large body of previous research has illustrated methods for optimizing the operation of existing microgrid resources, with a focus on microgrids with some form of energy storage [5–8]. Additionally, some researchers have investigated optimal system design for different types of microgrids in particular scenarios, such as grid-connected hospitals [9], standalone combined heat and power systems [10], as well as general formulations of standalone systems with multiple generators [11]. Much of the existing research in the field uses linear programming techniques to determine both the operation and design of the microgrid system, an approach that has both advantages and disadvantages. By using a linear programming approach, the truly optimal system design or operation can be determined. However, this approach normally accounts for neither the importance of uncertainty in load and variable renewable energy nor the risk aversion towards unserved load seen in the design of actual microgrids.

Because of the fundamental uncertainties inherent in microgrid design and operation, researchers have created battery and microgrid models of varying levels of complexity, depending upon the purpose for which the model will be used. Tradeoffs must be made between the complexity of the component modeling and the ability to search for optimal systems and system operation. In Bortolini et al., which also includes a thorough literature review of different microgrid modeling efforts, operational and economic elements of a grid-connected PV/battery system are investigated [12]. In this system, load is met first from the PV, then batteries, and the grid is used as a backup source. Batteries are never charged from the grid. In Khatib and Elmenreich, a generator/PV/storage system is considered in which load is met first from available PV energy, then from battery energy, and the generator is only started when PV and battery are unable to serve load [13]. When the generator is running, it is also used to charge batteries if possible. This approach easily answers the questions of when to operate the generator and when to charge the batteries from the generator, but does not allow a system designer to search for systems that can produce electricity at lowest cost, as cost is not part of the formulation.

Other models have used different approaches, focusing on particular elements of system components or operation. Dufo-López et al. use genetic algorithm search to identify optimal control strategy in addition to system design [14,15]. This permits their Hybrid Optimization by Genetic Algorithms (HOGA) model to co-optimize operation and system design and to search in a multi-criteria space that attempts to balance LCOE with life-cycle system emissions. However, the modeling of system components, especially energy storage, is necessarily quite limited. Koohi-Kamali et al. use agent-based modeling to investigate the use of PbA batteries to provide smoothing and other support services in a PV/diesel generator/PbA battery system [16]. They model the electrical and mechanical characteristics of the system in great detail, including elements such as generator torque versus crank angle and system active and reactive power. This extensive system model is used to demonstrate the operational value of energy storage providing integrating services.

With the Energy Systems Model (ESM), we create a versatile engineering-economic model of microgrid operation. We use this model to demonstrate that more sophisticated battery modeling can result in very different LCOE and system design, by comparing ESM to the popular microgrid modeling tool HOMER. We then use the ESM to investigate the economics and system design of Aqueous Hybrid Ion (AHI)-based microgrids in comparison to PbA-based systems.

HOMER is an easy-to-use system modeling program that utilizes a time-series (not linear programming) approach to microgrid operation. Originally developed by the National Renewable Energy Laboratory, HOMER can rapidly evaluate a variety of potential microgrid options [17]. HOMER is chosen as a comparison because it is commonly used in microgrid research, education, consulting and industry. HOMER Energy, the company that distributes the software, reports over 100,000 users in 193 countries [16]. While many other researchers have improved upon various aspects of HOMER's microgrid modeling, we demonstrate that more sophisticated modeling can result in very different results.

While HOMER has a relatively sophisticated and realistic modeling approach for most system components, its battery models are more theoretical to maintain ease of calculation. As a result, HOMER underestimates or neglects several important issues relating to battery operation in microgrid systems, such as capacity fade, temperature effects, or rate-based battery efficiency. We believe that the battery modeling is the weakest part of this useful modeling tool, and can be improved with a more realistic battery model.

Because we are particularly interested in the value and operation of batteries, we have developed our own Energy Systems Model (ESM) to evaluate the operation and costs of different standalone microgrid energy systems. Much of the modeling approach for ESM is similar to that used in HOMER, with improvements made where the HOMER approach appeared to lack the necessary sophistication. The ESM does not allow as many system elements as HOMER, which permits multiple generators and several different renewable generation technologies. Similar to HOMER and unlike much of the literature in the field of microgrid optimization, ESM uses operational algorithms that are risk averse towards unserved load. We believe that this better reflects the design and operation of actual microgrid systems.

One of the major reasons for creating the ESM was to evaluate and compare PbA batteries with Aquion's Aqueous Hybrid Ion (AHI) batteries in microgrid applications. AHI is a novel battery chemistry that offers durability across environmental and operational regimes, has a very high cycle lifetime, and a moderate capital expense. This makes AHI a potential improvement over the incumbent PbA technology, which has cycle life and operational limitations but a lower upfront cost.

This paper is structured as follows. In Section 2, we describe the structure and assumptions used in ESM. In Section 3, we compare ESM to HOMER, discussing the differences between the two programs, and provide an example of the effect that these differences have on output. In Section 4, we use ESM to evaluate and compare the economics of PbA and AHI batteries for standalone microgrid systems. Section 5 is a discussion of the implications of the results in Sections 3 and 4, and we conclude in Section 6.

2. Model description

At its core, the ESM is an engineering-economic model that inputs a particular microgrid system configuration, electricity load time series, and solar resource time series, determines the time-series operation of each component, and calculates the LCOE and other relevant financial information for the system. In the current

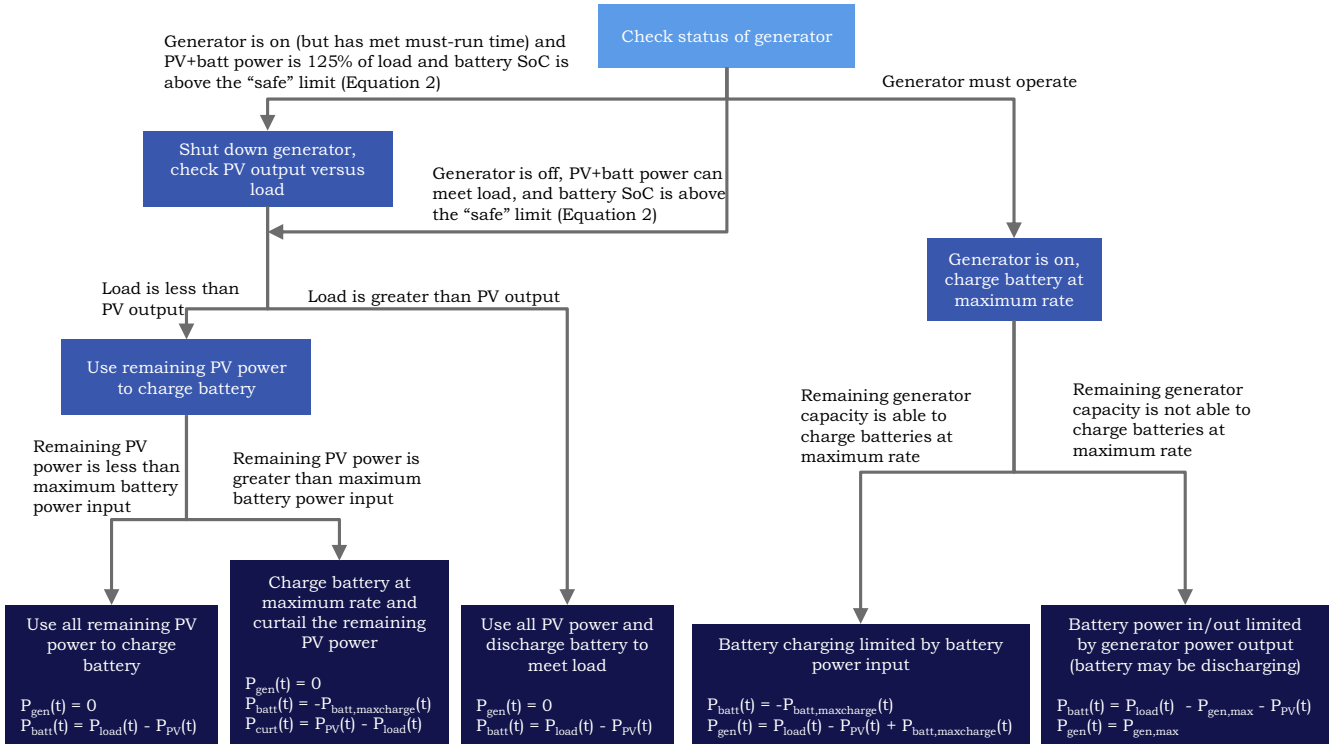

Fig. 1. Simplified flowchart of ESM decision making in scenarios where generator capacity is not sufficient to meet maximum load. The decision-making depicted in the flowchart is applied at each time step. Because the generator cannot always meet load, the system is operated in a conservative manner in an attempt to ensure sufficient battery capacity to meet expected future load.

version, the ESM is limited to systems with any combination of diesel generator, PV array, and battery energy storage. Higher-level functions of ESM can be used to choose an optimal system under a given set of input parameters (such as PV costs or diesel price) and can be used to study how changes in input parameters affect the optimal system configuration. The ESM is implemented in MATLAB and consists of approximately 5000 lines of code.

The ESM can input different amounts of installed diesel generation, solar PV,[1] and battery (either lead-acid (PbA) or Aqueous Hybrid Ion (AHI), though other chemistries or storage technologies could also be applied). The model is flexible enough that it can take any combination of system components as input, including cases where only one or two of these technologies are present. The ESM models a time-series operation of the components and attempts to choose a prudent output for the current time step without looking ahead at the actual future load or solar output. The model does use past operation to predict future operation, in a persistence-type forecast, by assuming that the upcoming 24 h period will have the same load and solar pattern as the previous 24 h period. This forecast of future load and solar output is used to determine whether excess generator capacity should be used to charge the batteries (see Figs. 1 and 2).

At each time step, the total power production must equal the load, as expressed in Eq. (1), where P_{load} is the power consumption of the load, P_{gen} is the power output of the diesel generator, P_{PV} is the power output of the PV system, P_{batt} is the power output of the battery, and P_{curt} is the curtailed or "dumped" power from the PV system. P_{batt} can be negative, indicating that the battery is charging. At each time step, the model preferentially uses all of the PV energy available, first to supply load and then to charge batteries if the PV is already satisfying the load. If there is still excess PV energy, it is curtailed or "dumped" and this curtailed energy is tracked with P_{curt}.

$$P_{load}(t) = P_{gen}(t) + P_{PV}(t) + P_{batt}(t) - P_{curt}(t) \quad (1)$$

The operation of the battery and generator depend on two factors: whether the generator is allowed to charge the battery,[2] and whether the generator is able to meet the maximum expected load. If the generator is unable to meet maximum load and is forbidden to charge the battery (an unrealistic case), then the battery is charged only from the PV, and the PV + battery attempt to supply load whenever that load is above the generator's maximum output. If the generator cannot supply maximum load but is allowed to charge the battery, it attempts to keep the battery at maximum charge whenever the generator is running, using any excess capacity to charge the battery.

In either of these cases, the diesel generator will shut down when the PV and battery are collectively able to supply the load, though in the case where the generator is not large enough to cover maximum load, the generator turns on again when the battery goes below a "safe" state-of-charge. The "safe" state-of-charge (SoC) is a function of both the amount that the generator is undersized relative to max load (a more undersized generator prompts a higher safe state-of-charge) and the average amount of dumped energy in the past (more dumped energy suggests that there is plentiful renewable energy to charge the battery, prompting a lower safe state-of-charge). Eq. (2) is used to calculate the "safe" battery charge state at each time step, where $E_{batt\ capacity}$ is the energy capacity of the battery, F_{safety} is a safety factor constant (set to 25 by default), $P_{dumped,avg}$ is the average dumped power over

[1] Actually, any zero marginal cost source works, including wind/solar combinations. The only limitation is that the time-series power output and costs of the energy source must be known.

[2] This is set at the start of the run, and users may have a different preference for different battery technologies. During optimization, the ESM examines both possibilities.

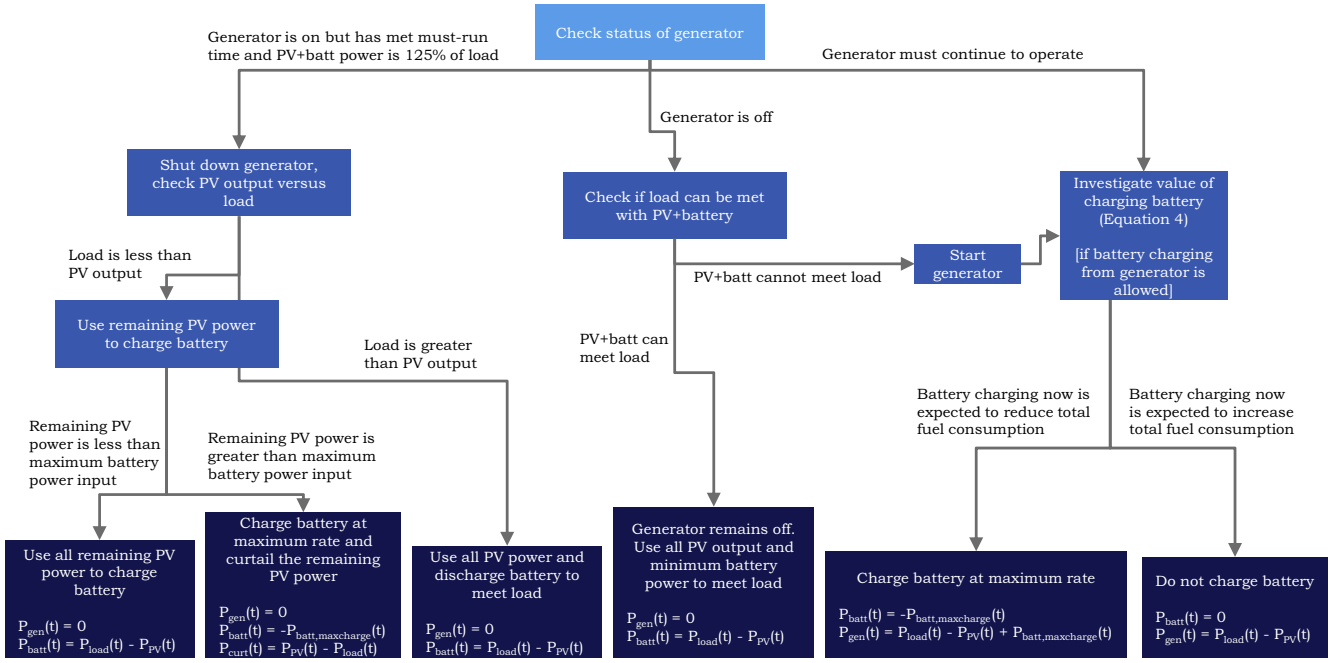

Fig. 2. Simplified flowchart of ESM decision making in scenarios where generator capacity is sufficient to meet maximum load. The decision-making depicted in the flowchart is applied at each time step.

the preceding 24 h period, and $F_{undersize}$ is an undersizing factor (ranging from 0 to 1) expressing the fraction of maximum load that can be met by the generator (Eq. (3)). Eq. (2) limits the safe SoC to have a maximum of 50%. A flowchart depicting the ESM decision-making in scenarios where the generator cannot meet maximum load is shown in Fig. 1.

$$E_{batt,safe}(t) = \frac{E_{batt\ capacity}}{2} - F_{safety} * \frac{P_{dumped,avg}(t)}{F_{undersize}} \quad (2)$$

$$F_{undersize} = \frac{P_{load,max} - P_{gen,max}}{P_{load,max}} \quad (3)$$

If the generator is able to supply maximum load, then the system does not need be as conservative with battery operation. A flowchart of the ESM decision making for cases where the generator is able to meet maximum load is shown in Fig. 2. In the case where the battery is not permitted to charge from the generator, all charging energy comes from excess PV output, and the diesel generator will shut down when the PV and battery are collectively able to supply 125% of expected load between the current point in time and the expected time when PV output will supply 100% of load. This approach is used to prevent the generator from charging the battery just before the daily PV output begins, which would be a waste of fuel. The excess 25% capacity requirement is to prevent constant cycling of the diesel generator in periods where PV + battery are barely able to support load. ESM forecasts future load and PV output by assuming that they will both follow the same pattern as the day before. The model then determines whether the current battery SoC plus forecasted PV will be able to meet 125% of forecasted load between the current point in time and when PV is expected to be sufficient on its own.

When the generator is allowed to charge the battery, it does so if the battery is able to supply the average load ($P_{batt,maxdischarge} > P_{load,average}$, where $P_{load,average}$ is the average load over the prior 24 h) *and* the excess fuel used to charge the battery at that moment is less than the fuel saved in the future by the operation of the battery (taking into account efficiency losses). In other words, the generator is only used to charge the battery if there is an expectation that doing so may allow the generator to shut down in the future, producing a net fuel savings. This is usually the case, due to generators being more efficient at higher power output, but highly inefficient (round trip efficiency < 50%) batteries can make battery charging from the generator unattractive. The net expected fuel use from charging is calculated using Eq. (4), where F_{net} is the expected net fuel consumption from charging the battery, $P_{batt,max}(t)$ is the maximum rate of battery charging at time t (limited by either the net generator capacity or the battery capacity), and η_{RTE} is the round-trip efficiency of the battery.

$$F_{net} = F(P_{load}(t) + P_{batt,max}(t)) - F(P_{load}(t)) - F(\eta_{RTE} * P_{batt,max}(t)) \quad (4)$$

In all scenarios, if there is ever a time step where the system is unable to meet load, the program stops the run and returns a signal that the studied system is insufficient. In other words, the load is considered completely inelastic and must be met. This and other conservative assumptions about microgrid operation were developed through discussions with actual microgrid developers.

The component modeling in ESM is described briefly below, with greater detail available in Appendix A. Additionally, the full ESM code is offered as open-source software to interested parties.

2.1. Battery modeling

The ESM was created to compare the value of energy services provided by PbA and AHI batteries. To accomplish this, a separate model was created for each technology to better reproduce their actual operational capabilities and limitations.

There are many factors affecting the performance and lifetime of PbA batteries [18], and microgrid and battery modeling efforts have used a variety of approaches to model their operation. Guasch and Silvestre offer a complex PbA battery model that includes many of the behaviors of PbA batteries and provide a method of populating the many model parameters through battery testing and cycling [19]. This work also proposes a state-of-health indicator for the battery that includes both temperature and working

zone elements and is similar to the capacity degradation model used in ESM. Dufo-López, Lujano-Rojas, and Bernal-Agustín investigate four different operational models and three different lifetime models for PbA batteries [20]. They compare modeled PbA lifetimes to actual lifetime of PbA batteries in two off-grid PV/PbA battery deployments with large battery banks experiencing slow and sometimes infrequent cycling. They find that the Schiffer method, a sophisticated approach using modeling of battery materials and chemistry [21], is most accurate for prediction of lead-acid lifetime and that other approaches tend to overestimate effective lifetime.

HOMER uses a two-tank kinetic battery model [17]. The two-tank kinetic model is an elegant simplification of battery operation that includes some observed battery behaviors, such as decreased effective capacity of batteries at higher charge rates. However, it is a simplification and does not correctly account for several important elements of battery operation (illustrated in Section 3).

In the ESM, for both lead-acid and AHI batteries, inefficiency is divided geometrically between the charge and discharge cycles. This is done to correctly account for the effects of complex and non-symmetrical battery cycling, such as long charge cycles coupled with faster discharges. Eqs. (5) and (6) show the method used to calculate energy and power in and out of the batteries, where $E_{batt,out}$ is the energy discharged from the battery, η_{RTE} is the round-trip efficiency of the battery, and $E_{batt,in}$ is the charge energy put into the battery. Inverters are scaled to the maximum discharge rate of the batteries and have an efficiency ranging from 10% to 95%, varying as a function of the power being converted at that time step (inverter efficiency calculations are discussed further in Appendix A.2).

$$E_{batt}(t) = E_{batt}(t-1) - E_{batt,out}(t) * \sqrt{\eta_{RTE}} + E_{batt,in}(t)/\sqrt{\eta_{RTE}} \quad (5)$$

$$P_{batt}(t) = E_{batt}(t)/T_{step} \quad (6)$$

Lead-acid batteries are modeled with several constraints. The charge/discharge rate is limited to C/4, meaning that the maximum rate (in W) is ¼ of the stated capacity (in W h). Due to inefficiency, this would actually be slightly more than 4 h for a charge (ie, for a 1000 W h battery, maximum charge rate is 250/W, which takes more than 4 h because less than 250 W h of energy is stored in the battery each hour).

Capacity fade is an important issue for PbA batteries. Using the default parameters (see Table 1), ESM models the capacity of the PbA battery as decreasing by 0.023% for each full cycle equivalent. At this rate, the battery can achieve 900 cycles at 100% depth of discharge (or 1800 cycles at 50% DoD, etc.) before it is at 80% of original capacity. Once the battery reaches 80% capacity, it is replaced by an equivalent battery with the same properties. PbA battery efficiency is based on measured efficiency curves (Table A3 in Appendix A), and is a function of the charge/discharge rate. The round-trip efficiency (RTE) is 86% at the maximum rate of C/4, and 92% for a charge below C/24, and linearly interpolated using the data points in Table A3.

The performance and lifetime of lead-acid batteries are affected by temperature [18], and many lead-acid battery models include temperature effects. Lujano-Rojas et al. have found that including temperature effects on lead-acid batteries can result in a negligible change for some systems that experience moderate average temperatures [22]. However, many of the most promising regions for microgrids are in warmer developing countries, where these effects will be more pronounced. Temperature effects on PbA batteries are modeled in two ways: increased capacity fade at higher temperatures and decreased energy availability at low temperatures. The nominal capacity fade rate (0.023% per complete cycle) is doubled for every 10 °C above 25 °C, and halved for every 10 °C below that temperature. Energy availability is a function of both temperature and charge/discharge rate: at lower temperatures and higher rates, the available energy is reduced. The energy availability at each point in time is a 2-dimensional linear interpolation between the data points in Table A4 in Appendix A.

For AHI batteries, the operational characteristics are based on a standard 140 W h battery, used in the current Aquion "AE1" Alpha battery stacks. This battery is limited to 8 A charge/discharge rate, with efficiency based on measured data (Table A1 in Appendix A). The efficiency is a function of both the state-of-charge (SoC) and the charge/discharge rate of the battery, ranging from a RTE of 94% (at the highest SoC and lowest rate) down to 34% (at the lowest SoC and highest rate), though both of these conditions are outside of typical use cases. AHI battery round-trip efficiency is calculated at each time step and is a 2-dimensional linear interpolation of the data points in Table A1. AHI batteries do not exhibit any significant capacity fade with usage, and the model assumes that capacity is constant. In the model, AHI battery lifetime is limited to 10 years, after which it is replaced by an equivalent AHI battery. AHI batteries are currently under cycle testing and show more than 10,000 cycles with very little capacity fade. As accurate cycle life data become available, they will be integrated into ESM.

Measured AHI battery performance data supporting these input assumptions are provided in the Supporting Information. Demonstration of AHI performance is ongoing. For the sake of this paper we use our current best data, however, subsequent testing is ongoing and a separate manuscript currently under review for publication presents in-depth AHI performance data [23].

The battery model has been validated and calibrated against actual battery cycling, through least-squares scaling of the battery parameters (efficiency curves and voltage-SoC function). The

Table 1
Parameters used in the ESM.

Parameter	Value
Diesel price	$1.50/L
Discount rate	10% per year
Diesel generator capital cost	$500/kW
AHI capital cost	$600/kW h
PbA capital cost	$200/kW h
PV capital cost	$4000/kW
Inverter capital cost	$350/kW
Diesel generator lifetime	10 years
PV lifetime	15 years
Inverter lifetime	15 years
Diesel generator must-run time	30 min
AHI maximum charge/discharge rate	8 A
AHI battery lifetime	10 years
PbA capacity fade	0.023% per complete cycle equivalent
PbA replacement	At 80% of original energy capacity

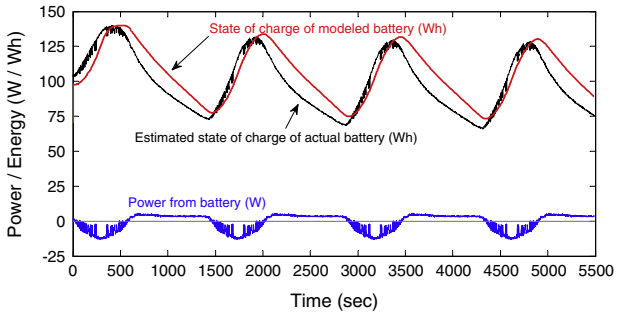

Fig. 3. State of charge of actual and modeled AHI batteries under a fast-charge/slow discharge cycle. The charge state of the actual battery is estimated from its voltage. The appearance of a time shift between actual and modeled AHI batteries is due to charge polarization of the actual battery, which increases the apparent charge state during charging and decreases the apparent charge state during discharge.

resulting adjusted values were checked against more complex and realistic cycling patterns of actual AHI batteries. Fig. 3 gives an example, comparing the modeled energy state of an AHI battery with the estimated energy state of an AHI battery under the same charge/discharge profile. The charge state of the actual AHI battery cannot be directly measured and is estimated from the voltage of the battery using voltage/SoC curves (determined from other testing). The actual battery is similar to the modeled battery, but demonstrates some charge polarization which shifts the curve up or down depending on the current charge/discharge state of the battery.

2.2. Cost calculations

The costs calculations are performed after the operational part of the model is complete. A Net Present Value (NPV) approach is used for cost calculations. Discounting is applied on a daily basis, both to correctly accommodate very high discount rates (if applied by the user) and because the model requires whole numbers of days of operation. The NPV of recurring operating costs, such as diesel fuel, are easily calculated using standard discounting calculations. Capital costs are handled by calculating the daily payment on the capital, amortized over the life of the unit. This essentially imagines that loans are taken out for each capital expense at an interest rate equal to the user-defined discount rate. These daily payments are then discounted at the discount rate. While this may appear to be an overly complex way to approach capital costs, this method allows a fair NPV comparison of capital cost with operating cost in those cases where the actual timeframe studied using time series data (days to weeks) is much shorter than the functional life of the capital investment (years). Note that while cost calculations assume that a loan is taken out for the capital investment, this does not have to be the case – this structure is just a way of calculating the equivalent daily capital cost. In other words, the purchasing entity should be indifferent between paying the capital costs upfront and taking a lifetime loan at an interest rate equal to their discount rate. Diesel generators and PV panels are modeled as having a fixed lifetime regardless of their operation.

The ESM outputs a variety of useful cost information about the resulting system, including levelized cost of electricity (LCOE), net present cost (NPC), upfront and average operating costs divided by system component, and payback period relative to a generator-only system. In the results below, we focus on LCOE rather than NPC, as LCOE is inherently normalized for system scale and is comparable with other systems (such as HOMER) which use LCOE as a primary decision variable. Furthermore, because of the simplifying assumption that discount rate equals interest rate, relative ranking by LCOE is always the same as the ranking by NPC.

2.3. Input data

For all scenarios discussed in this paper, the load and PV power inputs are eighteen days of actual 1-min resolution data from an existing microgrid system on an island in Southeast Asia, though any load profile can be used in ESM. The load has an average power of 81 kW, a maximum of 160 kW, and a minimum of 41 kW. Load follows the expected daily cycle with peak load occurring in the evening. The solar PV array has a 16% capacity factor, experiencing a mix of good and poor solar days, including several days in a row of very little PV energy production. As might be expected, weaker solar inputs result in lower PV utilization by the system. While the ESM is capable of modeling varying temperature effects, a fixed temperature of 30 °C is used throughout the analysis.

AHI battery cost used in the model is $600/kW h. This value is higher than the anticipated price when full scale production of this technology is established. The most important assumptions and inputs are listed in Table 1.

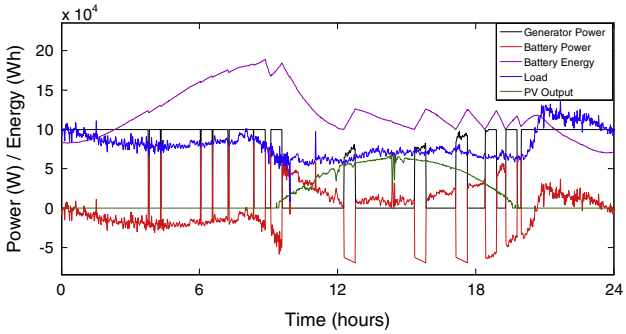

Fig. 4. Example output from the ESM, showing 1 day of operation of a 100 kW diesel generator, a 200 kW h AHI battery, and an 88 kW PV array providing electricity to a 160 kW max/81 kW average load.

2.4. Example output

Fig. 4 shows an example output from the ESM, with a 100 kW diesel generator, a 200 kW h AHI battery, and an 88 kW PV array providing electricity to a 160 kW max/81 kW average load. In this system, the generator is almost always at either maximum output (the most efficient operating point) or off. During the day, the generator shuts down except for a few short periods when the battery energy drops below the "safe reserve" level. The LCOE for this system is 44.7 cents/kW h, with 32.0 cents/kW h due to the generator and fuel, 8.0 cents/kW h due to the costs of the PV array, and 3.7 cents/kW h for the AHI batteries.

2.5. Sensitivity analysis and optimization

The ESM has higher-level sensitivity analysis and optimization routines that examine the effect of changes to the system parameters (scale of PV, generator, battery, and "generator charging" binary) and help to choose the best system under a given set of parameters and limitations. The optimization routine uses a combination of brute force, simulated annealing, and neighborhood search to determine the microgrid systems with the lowest LCOE. Most of the optimization is done by the simulated annealing routine, which is a serial optimization routine that starts as a "random walk" and becomes increasingly unlikely to transition to higher-LCOE systems. In addition to global optimization, a constrained optimization can also be performed where one or more of the system parameters (example: generator size) are held constant. Sensitivity analysis is performed by adjusting one or more input parameters and running a new optimization under the modified parameter set. The sensitivity analysis and optimization structure is described in greater detail in Appendix A.

3. Comparison of ESM to HOMER

HOMER is a useful modeling tool for investigating the scaling and operation of off-grid systems, but has several weaknesses that result in a favorable outlook towards the batteries that it models. This is driven by a few unrealistic assumptions and modeling approaches: the lack of battery capacity fade in the operational model, optimistic PbA battery lifetimes, lack of temperature effects in the battery model, the use of a constant round-trip efficiency, and a modeling resolution of 1-h. In this section, we discuss the effect that each of these has on LCOE and compare the output of ESM and HOMER. To accomplish this, we modified the ESM to operate with assumptions similar to HOMER and demonstrate that

it gives very similar results. Then we change the ESM assumptions back to their standard form (one at a time), showing how each change affects LCOE and system design. The discussion and comparison below are focused on PbA batteries because this is the only energy storage technology currently included in the built-in HOMER battery models.

3.1. Lack of battery capacity fade in the operational model

In actual operation of a PbA battery, the capacity of the battery will decrease over time until the battery is replaced (often assumed to be at 80% of original capacity). Just before replacement, a battery will be at a lower capacity and is unable to provide the same energy service that it could when new. For example, if a battery is replaced when it falls to 80% of original capacity and microgrid operation requires a certain battery capacity, the battery must initially be oversized by 25% to maintain the desired capacity at the end of the battery's life. HOMER does track capacity fade and uses it to determine when the batteries in a given system need to be replaced, but it does not include this in the operational model of a battery. For simplicity, it instead assumes that the battery operates to the original specifications throughout its lifetime, and thus underestimates levelized costs due to batteries costs by around 20%. This value works out to less than 25% (the amount of extra battery needed to ensure a minimum capacity at replacement) because oversizing a battery by 25% tends to improve the overall system operation and lower other system costs. For example, a larger battery will be more efficient due to lower charge rate per cell, can store more renewable energy, and allows for slightly more efficient generator operation.

3.2. Overly optimistic PbA battery lifetimes

The PbA battery data used in HOMER is based on manufacturer-reported lifetimes at different depths of discharge (DoDs), but these lifetimes normally require favorable operation of those batteries. HOMER's battery model states that a Hoppecke OPzS PbA battery will last 9 years under daily 50% DoD cycling or 15 years when cycled continuously at 20% DoD. But a lifetime of this magnitude from a PbA battery requires controlled operation of the batteries, such as limited charge rates, limited weekly cycling, occasional re-conditioning of the batteries, and controlled temperature, none of which are included in HOMER's modeling. For example, the Hup Solar One battery, a high-performance PbA system, comes with a 10 year warranty. But this warranty includes significant limitations, such as limiting use to 4 cycles per week and 210 cycles per year, charging at rate of C/5 to C/10, installation of a metering system, and operation within specific temperature ranges [24]. These limitation are not included in the HOMER battery model, and would complicate the use of PbA batteries in some energy systems. High-performance PbA batteries can last 10 or more years, but this lifetime is not possible without careful operation.

3.3. Lack of temperature effects

At higher temperatures, PbA batteries experience faster degradation [18]. At lower temperatures, their ability to deliver energy is reduced. HOMER accounts for neither of these effects. The ESM models temperature effects by assuming capacity fade is doubled for every 10 °C above 25 °C. In a realistic diesel/PV/battery system,[3] ESM estimates that a temperature increase of 5 °C results in a 17% higher levelized cost of electricity (LCOE) and a 42% increase in the costs due to PbA batteries (from 20.7 cents/kW h to 29.4 cents/kW h).

In some microgrids, batteries can be stored in a climate-controlled area at little or no cost, and temperature effects would not be a concern. But many of the applications for off-grid systems are in warmer areas of the world without easy access to climate control. While it is possible to add a climate control system for PbA batteries in hot environments, HOMER does not include this in the system model. The costs and power consumption of such a system would have to be added to the results. However, estimating the costs and load resulting from a climate control system is complicated because they are both affected by the design of the battery storage facility, which itself may be a compromise between climate control power consumption, capital costs, and battery performance. Because HOMER includes neither the temperature effects on batteries nor the cost of climate control, it is unable to accurately represent any battery operation scenario in climates that diverge from standard battery operating temperatures.

3.4. Use of a constant round-trip efficiency

HOMER uses a round-trip efficiency (RTE) value that is constant, while most storage technologies have an efficiency that is a function of charge/discharge rate and other factors. By making this assumption, HOMER neglects the fact that systems with heavily cycled batteries will result in a lower RTE and require either larger batteries or larger energy sources in order to meet the same load.

As an example, we used ESM to model a system where PbA batteries are used to optimize the operation of a diesel generator (System is a 100 kW diesel generator and 400 kW h of PbA batteries providing power to a 127 kW max load.). In this application, the batteries are cycled at high charge/discharge rates and a constant RTE underestimates the cost due to batteries. When a variable RTE (based on the charge/discharge rate) is used in ESM rather than an average RTE (the RTE for a 12-h rate), the fuel consumption increases by 60%, driving the overall system costs up by 40%. This result is extreme because this system operates the batteries at higher rates (up to C/4) almost all of the time, which is uncommon. But any system that spends more time operating at higher rates will result in an underestimate of battery or fuel costs from HOMER.

3.5. Modeling resolution of 1 h

HOMER uses a time resolution of 1 h for system operation. This resolution allows HOMER to examine daily variability while being able to quickly run many scenarios. But there are relevant sub-hourly phenomena, such as variability in load and PV output that are "averaged out" at an hourly level. For example, when the 1-min resolution load data we use is averaged out to 1-h and only a diesel generator is used to meet load, HOMER reports that the average LCOE is 39.9 cents/kW h, while the ESM reports that it is 39.7 cents/kW h. But when the original 1-min data are used and no other changes are made to the modeling, the ESM reports an LCOE of 50.3 cents/kW h. This 25% increase is due to two effects: the need for a larger diesel generator to meet the actual maximum load,[4] and increased fuel consumption due to sub-hourly fluctuations.[5]

[3] System is an 80 kW diesel generator, 260 kW of PV, and a minimally-sized PbA battery providing power to a 127 kW max load. At 25 °C, a 967 kW h PbA battery is needed. At 30 °C, a 1025 kW h PbA battery is needed.

[4] When data are averaged hourly, the maximum load necessarily decreases as a function of the short-term variability. The 1-min resolution load data have a maximum power of 159 kW. When averaged to 1-h resolution, the maximum decreases to 127 kW. The difference is due to occasional periods where the load will increase to 150 kW or more for a few minutes.

[5] Because the fuel efficiency curve of a diesel generator is convex (decreasing more rapidly at lower power output levels), an average power output always has a higher efficiency that the average of the efficiencies at the actual power output levels (unless the power output is constant). Thus, a generator with an output that fluctuates symmetrically around an average value over an hour will use more fuel than a generator that operates at that average value for an hour.

For a more complex system with a diesel generator, PV array, and batteries, the effects of changes in time resolution are smaller but relevant to battery modeling. In a example diesel/PV/PbA battery system with a large amount of solar,[6] switching from 1-min to 1-h resolution increases LCOE by only 3%. But the optimal amount of batteries in this system at a 1-min resolution is more than double (236%) the optimal amount at a 1-h resolution. By examining systems at a 1-h resolution, any microgrid modeling package will overestimate the capabilities of energy storage in the presence of fluctuating photovoltaics, and underestimate the amount of storage required. Furthermore, forecasting error for PV output will be much higher at 1-min resolution than at 1-h resolution [25], making the design of forecasting techniques becomes more important when higher time resolution is used.

3.6. Example of combined effects

While each of the factors described above are individually minor, they can add up to a significant difference in results. Not all of these will apply for a given system (for example, systems in climate controlled locations will not encounter temperature effects, and the use of a constant RTE is valid for PbA batteries cycled near average rates). However, several will apply for most realistic examples. To illustrate this, we start with a modified version of the ESM that uses the same modeling approach as HOMER, then introduce the more complex modeling elements one at a time and observe the change in estimated LCOE. Our example diesel generator/PV/PbA battery system uses a 100 kW diesel generator, 127 kW PV array, and 400 kW h of Hoppecke 8 OPzS 800 PbA batteries to meet a load with max power of 158 kW (in 1-min resolution) or 127 kW (in 1-h resolution). For this system, HOMER estimates the overall LCOE as 40.7 cents/kW h and the cost due to batteries as 3.4 cents/kW h. When using the same modeling approach and assumptions as HOMER, the ESM estimates the overall LCOE as 40.4 cents/kW h, with PbA batteries accounting for 3.3 cents/kW h. But as the ESM modeling approach is slowly adjusted, the LCOE increases to 44.1 cents/kW h and costs due to batteries rise to 7.0 cents/kW h (Fig. 5).

The assumptions are changed in the order shown in Fig. 5, from left to right. Reducing the battery lifetime throughput from 1713 complete cycles to 1400 complete cycles (to account for the non-ideal cycling profiles the battery is exposed to) increases the averaged cost of the batteries by 0.6 cents/kW h. Adding capacity fade into the operational model (rather than just the cost model) increases averaged cost of the battery by another 1.0 cents/kW h. Increasing ambient temperature from 20 °C to 25 °C to represent operation in a warmer climate increases averaged costs of the batteries by 1.8 cents/kW h. Modeling efficiency that varies by charge/discharge rate rather than as a fixed efficiency results in an increase of 0.1 cents/kW h. Finally, using a time resolution of 1 min rather than 1 h increases the averaged battery costs by 0.2 cents/kW h.

This example illustrates the importance of battery modeling assumptions, where more realistic modeling more than doubles the battery cost. Fig. 5 gives one example of how these assumptions affect system costs, but the effect of these assumptions will vary significantly between different energy systems, depending on system design and load patterns. More sophisticated modeling is not always superior, but we believe that ESM has a more realistic modeling approach for batteries operating in microgrid systems.

The increase in levelized battery costs from this example is more than 100%, but the LCOE changes from 40.4 cents/kW h to only 44.1 cents/kW h (9% increase). The effect that these modeling assumptions have on overall LCOE is relatively small, indicating that they have little effect on estimating overall system costs. However, for users that are particularly interested in energy storage economics, HOMER's modeling of storage may be skewed towards underestimating the costs due to batteries and result in sub-optimal microgrid system design.

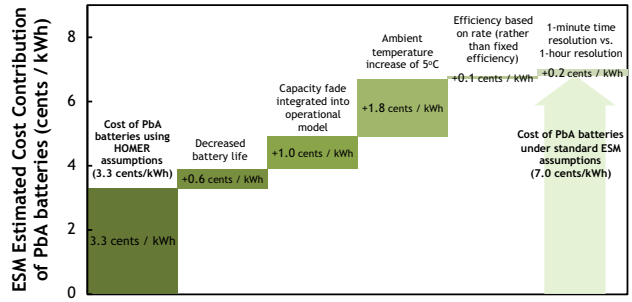

Fig. 5. Estimated cost of batteries in example diesel generator/PV/PbA battery system as modeling assumptions are modified, as estimated by ESM. Under assumptions similar to those used in HOMER, ESM gives an estimated battery cost contribution of 3.3 cents/kW h (compared to HOMER's estimate of 3.4 cents/kW h). ESM uses a set of assumptions that account for several important details of PbA battery operation. When these are included, the battery costs increase to 7.0 cents/kW h (or 5.2 cents/kW h without the temperature adjustment). ESM estimates overall system LCOE at 40.4 cents/kW h when using the same assumptions used in HOMER (HOMER estimates LCOE for this system as 40.7 cents/kW h). Under the more realistic assumptions, LCOE increases to 44.1 cents/kW h.

4. Comparing lead-acid and Aqueous Hybrid Ion batteries in ESM

In addition to its ability to calculate the LCOE of different microgrid systems, the ESM can be used to investigate a variety of higher-order questions about battery valuation and optimal system design under different scenarios and limitations.

Table 2 shows the optimal microgrid system design, levelized cost of electricity (LCOE), and net present cost (NPC) under a variety of system design limitations. With the base-case parameters and the standard load and PV profiles, the best system under either battery technology uses an undersized generator with a battery to provide peaking capability and a relatively small PV array to defer some fuel use. Under either battery technology, running only a diesel generator is more expensive than a diesel/battery system, a system where the generator is constrained to equal maximum load, or the optimal generator/PV/battery system. The last two rows of Table 2 show the optimal system when a diesel generator is not permitted. The "PV/battery only" row gives results with the actual PV data (described above), while the "Perfect PV/battery only" row uses a synthesized PV power output time series that has a perfect, cloudless pattern – the ideal PV energy production. The significant differences between these two rows illustrates the costs associated with unreliability of the solar energy source. The actual PV input data has several days in a row of very little energy production, resulting in a system that uses three times as many solar panels and five times as many batteries as the "perfect PV" system, in order to meet the same load. The PV/battery system is the only system more expensive than diesel-only.

Fig. 6 shows the LCOE of optimal AHI and PbA systems at various diesel prices. At a low diesel price of $0.50/L, no PV is used for either battery technology, and PbA batteries are a cheaper option. As the diesel price rises, for either technology, the ESM chooses to offset more of the diesel generation with solar PV energy. As the quantity of PV in the system increases, the need for storage also increases and more batteries are purchased. The differences

[6] 159 kW max load at 1-min resolution, 127 kW max load when averaged to an hourly resolution. System is a diesel generator, 126 kW PV, and batteries. The scale of the generator and batteries are optimized for lowest system LCOE.

Table 2
The optimal microgrid system, identified by ESM system optimization under various constraints and using the base-case values for all parameters. The "perfect" PV/battery system has the same constraints as the PV/battery system except that the PV output is a nearly perfect, cloudless pattern for the entire duration of the modeled period.

	AHI					PbA				
	LCOE (cents/kW h)	Net present cost ($)	Generator size (kW)	PV array size (kW)	Battery size (kW h)	LCOE (cents/kW h)	Net present cost ($)	Generator size (kW)	PV array size (kW)	Battery size (kW h)
Overall best system	54.75	3,533,000	96,700	127,600	189,900	58.99	3,806,000	104,600	128,600	219,400
Generator only	71.63	4,622,000	159,500	0	0	71.63	4,622,000	159,500	0	0
Generator/battery only	58.33	3,764,000	92,200	0	173,600	63.62	4,105,000	85,400	0	1,107,700
Generator constrained to equal maximum load	63.06	4,069,000	159,500	170,300	286,500	66.07	4,263,000	159,500	136,000	100,600
PV/battery only	197.37	12,736,000	0	962,800	8,134,300	210.09	13,557,000	0	906,200	16,820,400
"Perfect" PV/battery only	54.92	3,544,000	0	392,700	1,705,500	82.94	5,352,000	0	357,200	3,099,100

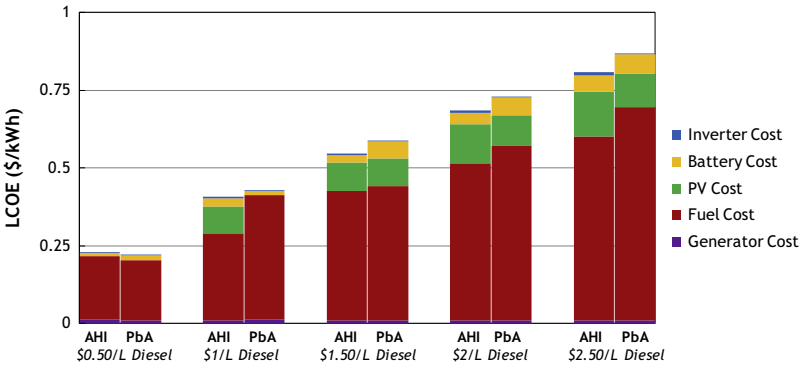

Fig. 6. LCOE of optimal AHI and PbA systems at various diesel prices. Each bar is broken into costs due to inverter, battery, PV, fuel, and diesel generator. The difference between AHI and PbA is amplified at higher diesel prices because the batteries are worked harder as more PV is added to the systems.

between AHI and PbA are amplified as diesel price is increased. This is because there are more batteries at higher diesel prices and these batteries are cycled more frequently, due to increased PV energy use. While the ESM allows for diesel to be eliminated from the system completely, it does not choose to do so because of the intermittent solar resource. There are several consecutive days of poor solar production and keeping the generator in the system is still the best option. However, the increase in PV/batteries displaces much of the diesel generation in the cases where diesel is more expensive. When diesel is $2.50/L, the optimal system consumes about half as much diesel as it does when the price is $0.50/L.

Fig. 7 shows LCOE for AHI and PbA systems at different PV prices. Decreasing the PV price results in decreased fuel usage, increased PV and battery deployment, and overall decreased prices. But the decrease in PV prices does not drive as much system changes as increases in diesel price (see Fig. 6). For example, decreasing the PV price from $4/W to $1/W results in less than a doubling of installed PV for either storage technology. The issue is partly that installation of PV has diminishing returns: when a small amount of PV is added to a generator system, the PV energy can be directly used to offset diesel consumption. As more PV is added, the excess solar energy must eventually be stored, requiring more batteries, which are themselves subject to efficiency losses and significant capital costs.

Fig. 8 shows the effect of temperature on the LCOE of optimal systems. As the average temperature of the battery environment increases, PbA systems become more expensive due to faster degradation of the batteries. In reality, a system developer may want to install a climate control system for the PbA batteries to

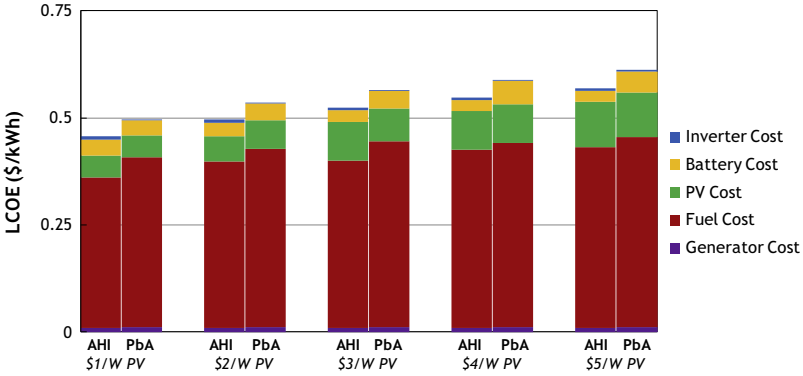

Fig. 7. LCOE of optimal AHI and PbA systems at various PV prices. Each bar is broken into costs due to inverter, battery, PV, fuel, and diesel generator. Even though the total cost of PV decreases at lower PV prices, the systems with lower PV prices have more installed PV (at a lower unit cost).

control the battery degradation. This decision, and the costs of temperature control for the batteries, are not considered in the ESM.

Fig. 9 shows the LCOE of AHI and PbA systems at different discount rates. Higher discount rates tend to favor PbA for two reasons. First, the batteries themselves are less capital intensive than AHI. Second, optimal PbA systems tend to rely less on PV/batteries and more on diesel generation than AHI. At higher discount rates, the PbA systems eliminate the PV completely and replace it with increased diesel use, which mainly results in operating costs rather than an upfront capital costs.

Fig. 10 compares the average daily battery cycling in optimal AHI and PbA systems. In almost all cases, the optimal system configurations result in greater cycling of AHI batteries. Across the 25 scenarios examined in Figs. 6–9, the AHI batteries were cycled an average of 72% more each day. This is because overuse of PbA batteries will cause capacity fade, while AHI does not have a similar constraint.

Fig. 11 shows the LCOE advantage of AHI versus PbA as a function of average battery cycling. Under conditions that prompt increased operation of batteries, such as greater amounts of PV in the system, the LCOE advantage of systems with AHI batteries tends to be increased. PbA batteries are preferred in systems where the batteries are lightly used.

All of the results above demonstrate that the optimal AHI system has a different design than the optimal PbA system. To illustrate the importance of this difference, the ESM was used to calculate the LCOE of a series of microgrid systems that were optimized for PbA but use AHI batteries instead. In each case, the PbA batteries are replaced by an equal capacity of AHI batteries. This essentially imagines AHI as a "drop-in replacement" for PbA microgrid systems. Table 3 shows the percent increase in LCOE for these systems, relative to the optimal AHI system under those prices. These systems have an LCOE that is 8–26% higher than the optimal AHI system and 0–16% higher than the optimal PbA system (not shown). These increases in LCOE represent the cost of inefficient system design, and show the importance of redesigning microgrid systems for new storage technologies rather than treating them as equivalent drop-in replacements.

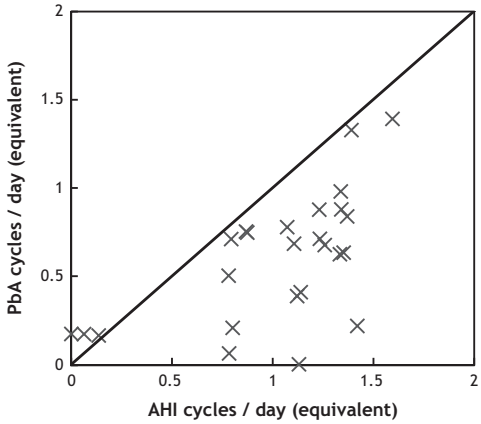

Fig. 10. Average cycles per day for optimal AHI and PbA systems at different diesel and PV prices. Each X corresponds to the optimal system at a different PV/diesel price combination (PV prices were $1, $2, $3, $4, and $5/W; diesel prices were $0.50, $1, $1.50, $2, and $2.50/L). A cycle is defined as the delivery from the battery of its stated energy capacity. The batteries are almost never cycled to complete discharge and the cycling is mainly the result of many smaller discharges per day (example: five 20% discharges is equivalent to one "cycle"). The diagonal line indicates where the points would lie if PbA and AHI were cycled the same amount. Instead, the points fall predominately below the line, indicating that the optimal systems for AHI batteries tend to use the batteries more aggressively than the optimal PbA systems.

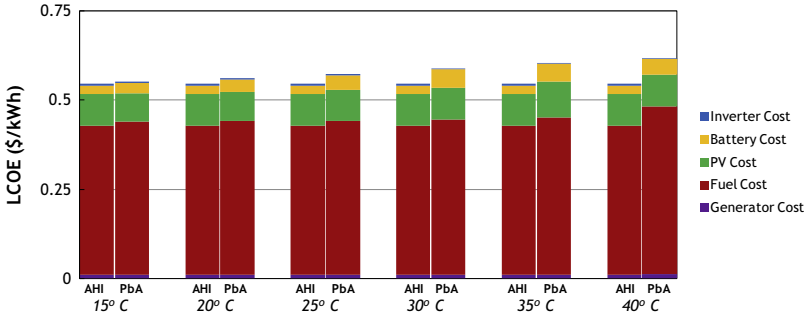

Fig. 8. LCOE of optimal AHI and PbA systems at various temperatures. Each bar is broken into costs due to battery, PV, fuel, and diesel generator. As temperature is increased, PbA capacity fade is accelerated, resulting in decreased lifetime and increased overall costs.

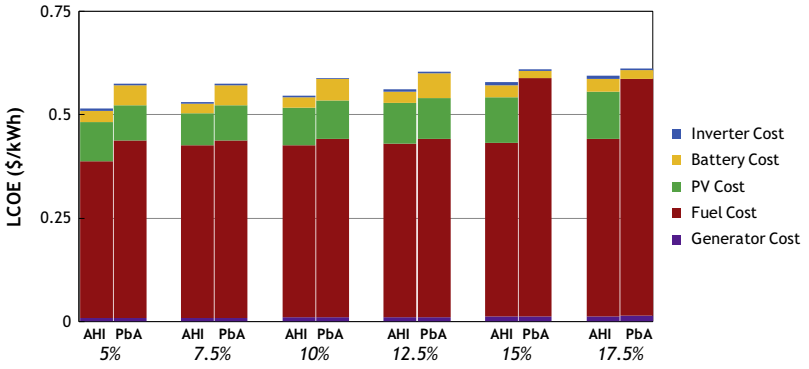

Fig. 9. LCOE of optimal AHI and PbA systems at various discount rates. Each bar is broken into costs due to battery, PV, fuel, and diesel generator. Because AHI is more capital intensive than PbA, lower discount rates favor AHI.

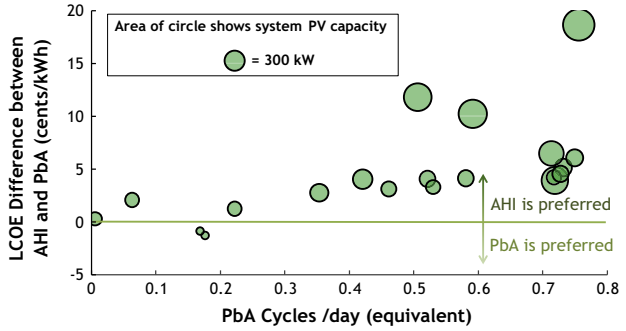

Fig. 11. LCOE difference between AHI and PbA versus average daily cycling of PbA batteries for 20 systems. Each circle corresponds to the optimal system at a different PV/diesel price combination (PV prices were $1, $2, $3, and $4/W; diesel prices were $0.50, $1, $1.50, $2, and $2.50/L). The area of the circle shows the quantity of PV for that system. A battery cycle is defined as the delivery from the battery of its stated energy capacity over any number of discharges. The batteries are almost never cycled to complete discharge and the cycling is mainly due to several smaller discharges per day (example: five 20% discharges is equivalent to one "cycle"). In conditions that favor stronger cycling of batteries, the advantage that AHI has tends to increase. This stronger cycling is partly a result of greater quantities of PV in the system.

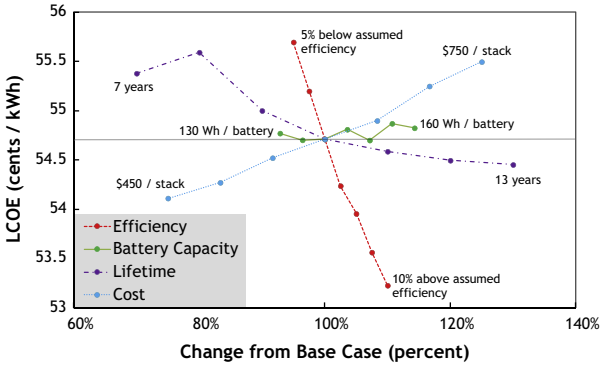

Fig. 12. Sensitivity plot of LCOE as AHI battery properties are changed. Each point represents a re-optimization of the generator/PV/battery system as the AHI battery properties are changed. Only one property is modified at a time, and each line shows the trend in LCOE change as a single battery parameter is modified from the base value. These results can be used to predict the value to a potential customer of different battery improvements. Steeper lines indicate parameters where small changes can result in larger LCOE improvements. All parameters except efficiency are a simple replacement of a single input. Because modeled battery efficiency changes as a function of rate and state-of-charge, efficiency changes are relative to the calculated efficiency at each point in the modeled operation.

Fig. 12 is a sensitivity plot of AHI properties, showing the change in optimal system LCOE as different battery properties are modified. The steeper lines indicate parameters where small changes in input assumptions result in large changes in system LCOE. The figure shows that efficiency improvements can cause particularly large LCOE improvements in AHI microgrids. Decreased cost and increased lifetime also contribute significantly to improved LCOE. Battery capacity increases do not result in improved LCOE because the system is power limited rather than energy limited.

5. Discussion

At least for the system configurations and load/PV profile investigated in this study, ESM estimates that AHI has a small LCOE advantage over PbA. There are a number of factors that contribute to this result. Most importantly, the longer lifetime of AHI batteries tends to bring their discounted costs to a level closer to PbA. But this does not account for the entire difference. At a 10% discount rate, amortized annual costs of one kW h of AHI over 10 years are still 20% higher than the amortized annual costs of one kW h of PbA that lasts 3 years. Because AHI batteries can be cycled more deeply and do not experience significant capacity fade, fewer nominal kW hs are needed to deliver the same energy service. This need for fewer nominal kW h of AHI to provide the same energy service as a larger PbA battery is an important element to the AHI battery economics.

In all of the examined scenarios, ESM estimates that the generator-only option was inferior to a generator/battery system. This is primarily due to the value of allowing the generator to be undersized and therefore more efficient. Because the generator efficiency decreases at partial load, full-size or oversized generators generally operate at an inefficient output, while an undersized generator can be operated at full output most of the time (see Fig. 4 for an example). This observation is dependent on a varying load profile, such as the one used in this work which has a peak load more than three times higher than minimum load. This load profile comes from an actual microgrid system, but other systems with more consistent load would prompt lower use of batteries for generator optimization. In real deployments, this "generator optimization" is generally not done with PbA batteries, as PbA systems are normally designed with a goal of reducing unnecessary battery cycling. AHI batteries are not negatively affected by continuous cycling and could provide this service effectively, but doing so would require microgrid developers to re-design their systems and to have confidence in the reliability and cycle life of the AHI technology.

AHI is not a drop-in replacement for PbA, and the results in Table 3 illustrate the importance of redesigning microgrid systems when changing between energy storage technologies. Across the many scenarios studied above, the optimal AHI system tends to use more solar PV and less diesel fuel than the optimal PbA systems. Additionally, the optimal AHI systems cycle the batteries 72% more than the optimal PbA systems. In order to extract the most benefit from AHI batteries, microgrid developers will need to create systems that exploit the different capabilities of AHI, a process that will require further testing and development.

Table 3
LCOE increase of AHI "drop-in replacement" systems relative to optimal AHI systems, for systems at different diesel and PV prices. "Drop-in replacement" refers to a system that has been optimized for PbA batteries (at a particular combination of diesel and PV prices), but where those batteries have been replaced with an equivalent capacity of AHI batteries. Because these system have been optimized for a different technology, the LCOE is higher than for an optimal AHI system in all cases, despite the results above showing that microgrids using AHI produce electricity at lower LCOE. The scenarios marked "Insufficient" are cases where the AHI drop-in replacement system is unable to meet load at all points in time.

LCOE increase		Diesel price				
		$0.50/L	$1/L	$1.50/L	$2/L	$2.50/L
PV price	$1/W	23%	19%	12%	17%	Insufficient
	$2/W	19%	20%	11%	Insufficient	26%
	$3/W	10%	18%	13%	8%	Insufficient
	$4/W	12%	18%	11%	9%	9%
	$5/W	8%	10%	13%	15%	8%

AHI batteries were found to have a larger LCOE advantage in scenarios where batteries are cycled more deeply and more frequently. As discussed above, the amortized costs of AHI are still significantly higher than PbA and AHI only has an advantage in systems where frequent battery cycling is valuable. In cases where batteries are used more for backup than constant cycling, PbA is a better choice. One example is a PV/battery system in a location with poor solar resource. In cloudy locations, there can be frequent several-day periods with very little energy coming from the PV panels and, without a generator, the batteries must be scaled so that they can meet load for several days in a row. This results in very large batteries that are lightly cycled most of the time, conditions that result in PbA being the superior choice.

6. Conclusions

ESM is a time-series microgrid modeling tool that is designed to perform realistic battery modeling and economic evaluation. The ESM structure is similar to the popular HOMER microgrid software, but attempts to improve upon HOMER's battery modeling approach. The ESM battery modeling includes important elements of battery operation such as operational capacity fade, variable efficiency based on charge rate, temperature effects, and fine time resolution. We compare the results of ESM and HOMER, and show that they produce similar results when ESM uses the same battery modeling assumptions as HOMER. However, ESM produces significantly different results under more realistic battery modeling.

ESM was used to study the economics and optimal system design of AHI-based microgrids, and these results are compared to PbA-based systems. Across several realistic scenarios, the ESM estimates that AHI-based generator/PV/battery systems have lower LCOE and NPC than PbA-based systems by a small margin, but with a higher upfront cost. AHI appears to be a better complement to solar PV in generator/PV/battery systems, and scenarios that favor the use of PV (low PV prices, low discount rates, and high diesel prices) tend to increase both the LCOE advantage of AHI and the optimal amount of deployed PV. Depending on the scenario, optimal AHI-based systems have a 5–20% lower LCOE and use 10–30% more PV than optimal PbA systems. The small advantage in AHI LCOE relies on identifying scenarios where frequent battery cycling is valuable. Applications that require batteries to serve as a backup energy service rather than a cycling service will find that PbA batteries are a better choice.

We also investigated the potential for AHI batteries to serve as "drop-in" replacements for PbA batteries in existing or pre-designed PbA microgrids. In these cases, when the microgrid is not designed in accord with AHI capabilities and limitations, AHI is a poor replacement for PbA, resulting in LCOE increases of 10–20%. Because of differing capabilities, microgrids using AHI batteries should be designed and operated differently than similar PbA microgrids.

7. A note on the Energy System Model

The authors offer the ESM as open-source software for use by other researchers or commercial entities involved in microgrid development. Any inquiries into the system should be directed to the corresponding author. As a "living" model, the ESM experiences frequent updates and improvements, incorporating new data or functionality.

Acknowledgments

The authors would like to thank Optimal Power Solutions for providing the microgrid load and PV data along with advice about the design and operation of microgrid systems. Funding for this research was provided by Aquion Energy.

Appendix A. ESM model structure

A.1. System operation

The core ESM model can input different amounts of diesel generation, solar PV (or any other zero marginal cost source, including wind/solar combinations), and battery. The model operation is flexible enough to account for any combination of these, including cases where only one or two are present, such as PV/battery or diesel/battery systems. The core ESM model outputs the time-series operation of the system elements and a set of financial calculations based on net present cost of system operation.

The model uses a time-series operation and attempts to choose the most prudent output for the current time step without any look-ahead. The model does use past operation to predict future operation, by assuming that the next day will look approximately like the previous day. However, the main focus of the model is meeting current load in the most efficient manner. This strategy does not necessarily result in a strictly optimal operation of the system, but better reflects a more conservative and realist operation of the system components, which we decided upon after discussion with microgrid developers.

At each time step, the model first uses all of the available PV energy, first to supply load and then to charge batteries if the PV is already satisfying the load. If there is excess PV energy, it is "dumped" and this dumped energy is also tracked (for reference only). The operation of the battery and generator depends on two factors: whether the generator is allowed to charge the battery (this is set at the start of the run, configurable by the user), and whether the generator is able to cover the maximum expected load. The maximum load is taken as the maximum load of the input load data – this is the one instance in which the model is permitted to "look ahead".

If the generator is unable to always supply load and cannot charge the battery (a somewhat unrealistic case), then the battery is charged only from the PV, and the battery attempts to supply net load whenever net load is above the generator's maximum output. When the generator cannot supply max load but is allowed to charge the battery, it attempts to keep the battery at maximum charge, using any excess capacity to charge the battery as long as the generator is running. In either of these cases, the diesel generator will shut down when the PV and battery are collectively able to supply the load, though in the case where the generator is not large enough to cover maximum load, the generator turns on again whenever the battery goes below a safe level (normally around 50% state-of-charge).

If the generator is able to supply maximum load, then the system does not need to be as conservative with the battery operation. In the case where battery is not permitted to charge from the generator, all charging energy comes from excess PV output, and the diesel generator will shut down when the PV and battery are collectively able to supply the load. When the generator is permitted to charge the battery, it does so whenever the battery is able to supply the average load *and* the excess fuel used to charge the battery now is less than the fuel saved in the future by the operation of the battery (taking into account efficiency losses). In other words, the generator should only be used to charge the battery if there is an expectation that doing so may allow the generator to shut down in the future *and* doing so would save some fuel (this is the case most of the time, but very inefficient batteries can make battery charging from the generator unattractive).

In the actual ESM model, the operation of the generator (based on all of the rules above) is determined first, then the PV and battery operation is calculated. The generator has a "must-run time", which is set at 30 min (though configurable by the user) and has no ramping limitations or low operating limit. The generator is modeled with a linear fuel consumption curve, and this curve is scaled linearly with generator size. The fuel consumption curve is defined in the following way: for every kW of generation capacity, the generator uses 0.34 L/h at maximum output and 0.125 L/h at zero output. Fuel consumption at intermediate outputs are interpolations between these two points.

In all cases, if the system encounters a point where it is simply unable to meet load, the program stops the run and returns a signal that the studied system is "insufficient". In other words, the load is completely inelastic and must be met for the entire study period.

A.2. Battery modeling

The ESM was created with the explicit intention to examine battery operation and economics for microgrids. The initial version of the ESM is focused on comparing AHI and PbA battery technologies. In order to achieve this, separate battery models were created for AHI and PbA batteries, reflecting the technical characteristics of the technology.

Battery inefficiency is split evenly between the charge and discharge cycles. As an example, at a round-trip efficiency of 80%, if you put 1 W h into the battery, 0.89 W h of energy is actually stored in the battery. When you take out that 0.89 W h, you actually receive = 0.8 W h, giving you the RTE of 80%. This strategy allows the model to account for differing rates for charging and discharging.

For AHI, the battery efficiency is a function of both the state of charge and the charge/discharge rate. Table A1 shows the round-trip efficiency (RTE) of AHI batteries used in the ESM. Actual RTE values are interpolations between the values shown in this table. The AHI batteries have a usable voltage range of 1.6–7.6 V, and a maximum current input/output of 8 A for each 140 W h battery pack. The AHI batteries do not experience any significant capacity fade or temperature effects, and these are omitted from the battery model.

Inverters are scaled to the maximum battery discharge and have an efficiency curve as shown in Table A2.

Lead-acid batteries have a maximum charge/discharge rate of C/4. Capacity fade of PbA is tracked in the model and adjusted at each time step. The capacity of the PbA battery decreases by 0.023% for each full cycle equivalent (ie, two 50% charge/discharges or ten 10% charges and a full discharge are all considered one "full cycle equivalent"). Once the battery capacity falls to 80% of the original capacity, it is replaced by an equivalent battery with the same properties. PbA capacity fade rate is doubled for every 10 °C above 25 °C, and halved for every 10 °C below 25 °C.

Table A1
Round-trip efficiency values for AHI battery, as a function of battery voltage and current. The operating voltage of an AHI battery ranges from 1.6 to 7.6 V, and the maximum suggested charge/discharge rate is 8 A. Towards top-of-charge, the battery efficiency drops to 1% as continuous energy input brings the voltage asymptotically to maximum charge. These data are for a battery with a 140 W h capacity.

	1.6 V	3.9 V	4.2 V	5.3 V	5.7 V	6.4 V	7.3 V	7.6 V
0 A	84.1%	90.5%	91.4%	92.5%	93.0%	93.1%	94.0%	1.0%
2 A	73.8%	81.8%	83.4%	85.1%	86.1%	86.7%	88.3%	1.0%
4 A	56.7%	70.7%	73.6%	76.5%	78.3%	79.3%	82.0%	1.0%
6 A	43.1%	61.3%	65.0%	68.7%	71.1%	72.5%	76.0%	1.0%
8 A	32.1%	53.3%	57.6%	61.8%	64.7%	66.3%	70.3%	1.0%

Table A2
Efficiency curve for inverters. Charge/discharge rate is relative to the maximum inverter power input/output, which is set to equal maximum battery power.

Charge/discharge rate	100%	80%	60%	40%	20%	0%
Efficiency	91%	92.3%	93.4%	94.5%	95.4%	10%

Table A3
Round-trip efficiency of PbA batteries as a function of charge rate.

Charge/discharge rate (C rate)	C/4	C/8	C/12	C/24
Round-trip efficiency	86%	88%	89%	91%

Table A4
Stored energy availability for PbA batteries as a function of charge/discharge rate and temperature.

	C/4 (%)	C/10 (%)	C/24 (%)
60 °C	83	99	108
50 °C	82	98	107
40 °C	81	97	106
30 °C	78	96	105
20 °C	75	92	101
10 °C	69	88	95
0 °C	63	80	88
−10 °C	53	70	77
−20 °C	45	55	63

PbA round-trip efficiency is a function of charge/discharge rate (Table A3). For charge/discharge below the C/24 rate, the 91% RTE value is used.

PbA also has limits on the available discharge energy based on temperature and charge rate – at higher rates and lower temperatures, some of the stored energy is unavailable (Table A4). As an example, at a rate of C/4 and a temperature of 20 °C, only 75% of the stored energy is available. This means that the battery cannot go below 25% state of charge at this temperature and rate. Since the system cannot control the temperature, the battery must discharge at a slower rate in order to access the stored energy. Some of the values in Table A4 are above 100%, indicating that the battery can discharge more than the nominal capacity of the PbA battery at higher temperatures and lower rates.

A.3. Cost calculations

The costs of operation are calculated after the operation phase is complete and an NPV calculation approach is used. Discounting is done on a daily basis, both to correctly accommodate very high discount rates and because the model requires whole numbers of days of operation. Capital costs are handled by calculating the daily payment on the capital, amortized over the life of the unit. This essentially imagines that loans are taken out for each capital expense at an interest rate equal to the discount rate, and that these loans are amortized and paid off daily. These daily payments are then themselves discounted at the discount rate.

Diesel generators, inverters, and PV panels are modeled as having a fixed lifetime regardless of their operation. AHI batteries currently have a fixed lifetime, regardless of operation. PbA battery lifetime is based on the capacity fade of the battery, and PbA batteries are replaced when capacity drops to 80% of original capacity.

A.4. Higher-level optimization and sensitivity analysis

The core ESM model inputs a set of parameters and a system design (a certain quantity of generator, PV, and battery, and a "generator charging allowed" binary) and calculates the operational

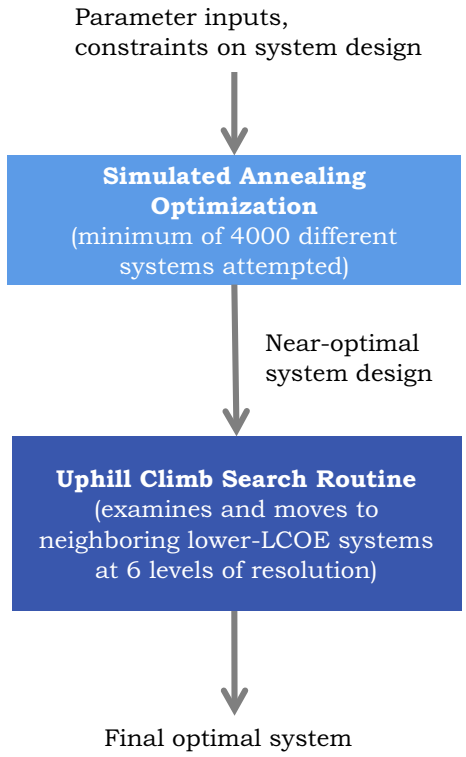

Fig. A1. Diagram of optimization routine used to identify optimal system designs for a given set of inputs.

and then the financial characteristics of the system. In many cases, the user is interested in finding an optimal system design with a given set of price and operational parameters or examining how the optimal system design (or other characteristics) changes as input parameters are changed. The high-level functions of the ESM model include routines that perform both of these operations.

ESM uses a combination of simulated annealing, uphill climb, and brute force optimization techniques to find optimal system design (Fig. A1). The ESM optimization routine first uses a simulated annealing algorithm to seek optimal system designs, given a particular set of inputs. It does this by first examining a "nearby" system to the currently chosen system. The optimizer has four parameters to vary: generator size, PV size, battery size, and a binary flag that determines whether the battery can be charged from the generator. The optimizer identifies a "nearby" system by choosing a random point that has a value within 5% of the current system for the three continuous variables and randomly chooses a 0 or 1 for the "generator charging" binary. If this "nearby" system has a lower levelized cost of electricity (LCOE), then the optimizer accepts the new system as the current choice (Eq. (A2)). If the new system has a higher LCOE, then the optimizer chooses it with a probability based on how much higher the LCOE is and how many runs have been completed (Eq. (A3)). In Eq. (A1), $T(x)$ is the simulated annealing "temperature", which decreases linearly from a starting temperature (T_o, set to 0.02) down to zero during the last run. Variable x represents the current run number and n is the total number of runs. Simulated annealing optimization was created in analogy to the annealing of metals, and the "temperature", which decreases monotonically, dictates the probability that the program will choose a system with higher LCOE. In (A2) and (A3), $P(transition)$ is the probability that the routine transitions to the new system over the currently chosen system. The user can input a "target time" (in s) for the desired duration of the system optimization. This time affects the number of examined systems (n, in Eq. (A1)) that the simulated annealing routine examines. However, we limit n to be greater than 4000 to allow the search routine to get to a near-optimum.

$$T(x) = T_o\left(1 - \frac{x}{n}\right) \tag{A1}$$

$$P(transition) = 1 \quad if\ LCOE(x) \leqslant LCOE(chosen) \tag{A2}$$

$$P(transition) = \frac{e^{[LCOE(x) - LCOE(chosen)]}}{T(x)} \quad if\ LCOE(x) > LCOE(chosen) \tag{A3}$$

At the start of the optimization, the search routine is very likely to transition to an inferior system, and is essentially a random walk. But as the optimization progresses, the ESM is increasingly likely to choose only systems that have a lower LCOE than the current choice. This allows the ESM to initially search a diverse and rugged terrain and eventually focus only on changes that improve LCOE. The simulated annealing search concludes with a system that is at least a local optimum and is likely to be close to the global optimum. Earlier attempts with "uphill climb" routines discovered that the search terrain is "rough" and that the best solutions border a forbidden area in the search space (where the proposed system is insufficient to meet load). This results in what is effectively a rugged Pareto frontier of possible best systems. When using the search parameters described above, the simulated annealing algorithm was able to efficiently traverse this frontier to the region of lowest LCOE.

Once the simulated annealing search has produced a result, further refinement of the system is done via a local "uphill climb" search. This search examines 54 ($3 \times 3 \times 3 \times 2$) nearby neighbors and then transitions to the one with the lowest LCOE that is also lower than the current LCOE. Neighbors are chosen by adding a small amount, subtracting a small amount, or not changing each of the three continuous variables and trying both values for the binary flag (Eq. (A4)). The delta values are determined using Eqs. (A5)–(A7)). If none of those 54 neighbors have a lower LCOE, then the system goes to the next level of resolution and examines all 54 neighbors at that level of resolution. When the system reaches the highest level of resolution (limited to six levels), it starts the entire process over at the lowest resolution level, and repeats this larger loop until it progresses through all resolution levels without a transition to a new system. This is performed in case fine tuning of the system at high resolution allows for larger changes to occur at low resolution.

$$S_i = S_i + \{0, Delta_i, -Delta_i\} \text{ for continuous variables} \tag{A4}$$

$$Delta_{gen} = \frac{P_{load,max}}{(3.1)^{r+1}} \tag{A5}$$

$$Delta_{PV} = \frac{20 * P_{load,max}}{(3.1)^{r+1}} \tag{A6}$$

$$Delta_{batt} = \frac{10 * 24 * P_{load,average}}{(3.1)^{r+1}} \tag{A7}$$

Sensitivity analysis is performed by changing one or more input parameters and then running a new optimization for each change in parameters. This allows the user to investigate, for example, the effect on LCOE of increasing diesel prices.

Appendix B. Supplementary material

Supplementary data associated with this article can be found, in the online version, at http://dx.doi.org/10.1016/j.enconman.2014.10.011.

References

[1] Murthy Balijepalli V, Khaparde SA, Dobariya CV. Deployment of microgrids in India. In: Power and energy society general meeting, 2010 IEEE; 2010.

[2] Katiraei F, Iravani R, Hatziargyriou N, Dimeas A. Microgrids management. IEEE Power Energy Mag 2008:54–65.

[3] Van Broekhoven S, Judson N, Nguyen S, Ross W. Microgrid study: energy security for DoD installations. Lexington, MA; 2012.

[4] New York State Energy Research and Development Authority. Microgrids: an assessment of the value, opportunities and barriers to deployment in New York State. Albany, NY; 2010.

[5] Celli G, Pilo F, Pisano G, Soma GG. Optimal participation of a microgrid to the energy market with an intelligent EMS. In: The 7th international power engineering conference, 2005. IPEC 2005, vol. 2; 2005. p. 663–8.

[6] Chen C, Duan S, Cai T, Liu B, Hu G. Smart energy management system for optimal microgrid economic operation. IET Renew Power Gener 2011;5(3):258–67.

[7] Katiraei F, Iravani MR. Power management strategies for a microgrid with multiple distributed generation units. IEEE Trans Power Syst 2006;21(4):1821–31.

[8] Tsikalakis AG, Hatziargyriou ND. Centralized control for optimizing microgrids operation. In: Power and energy society general meeting, 2011 IEEE; 2011. p. 1–8.

[9] Hawkes AD, Leach MA. Modelling high level system design and unit commitment for a microgrid. Appl Energy 2009;86(7–8):1253–65.

[10] Hernandez-Aramburo CA, Green TC, Mugniot N. Fuel consumption minimization of a microgrid. IEEE Trans Ind Appl 2005;41(3):673–81.

[11] Zoka Y, Sugimoto A, Yorino N, Kawahara K, Kubokawa J. An economic evaluation for an autonomous independent network of distributed energy resources. Electr Power Syst Res 2007;77:831–8.

[12] Bortolini M, Gamberi M, Graziani A. Technical and economic design of photovoltaic and battery energy storage system. Energy Convers Manage 2014;86:81–92.

[13] Khatib T, Elmenreich W. Novel simplified hourly energy flow models for photovoltaic power systems. Energy Convers Manage 2014;79:441–8.

[14] Dufo-López R, Bernal-Agustín J, Yusta-Loyo J, Domínguez-Navarro J, Ramírez-Rosado I, Lujano J, et al. Multi-objective optimization minimizing cost and life cycle emissions of stand-alone PV–wind–diesel systems with batteries storage. Appl Energy 2011;88:4033–41.

[15] Dufo-López R. iHOGA, November 2013 <http://personal.unizar.es/rdufo/index.php?option=com_content&view=article&id=2&Itemid=104&lang=en> [accessed September 2014].

[16] Koohi-Kamali S, Rahim N, Mokhlis H. Smart power management algorithm in microgrid consisting of photovoltaic, diesel, and battery storage plants considering variations in sunlight, temperature, and load. Energy Convers Manage 2014;84:562–82.

[17] Lambert T, Gilman P, Lilienthal P. Micropower system modeling with HOMER <http://homerenergy.com/documents/MicropowerSystemModelingWithHOMER.pdf>.

[18] Spiers D, Rasinkoski A. Predicting the service lifetime of lead-acid batteries in photovoltaic systems. J Power Sources 1995;53:245–53.

[19] Guasch D, Silvestre S. Dynamic battery model for photovoltaic applications. Prog Photovolt: Res Appl 2003;11:193–206.

[20] Dufo-López R, Lujano-Rojas J, Bernal-Agustín J. Comparison of different lead-acid battery lifetime prediction models for use in simulation of stand-alone photovoltaic systems. Appl Energy 2014;115:242–53.

[21] Schiffer J, Sauer D, Bindner H, Cronin T, Lundsager P, Kaiser R. Model prediction for ranking lead-acid batteries according to expected lifetime in renewable energy systems and autonomous power-supply systems. J Power Sources 2007;168(1):66–78.

[22] Lujano-Rojas J, Dufo-López R, Bernal-Agustín J. Optimal sizing of small wind/battery systems considering the DC bus voltage stability effect on energy capture, wind speed variability, and load uncertainty. Appl Energy 2012;93:404–12.

[23] Whitacre J, Shanbhag S, Mohamed A, Polonsky A, Carlsi K, Gulakowski J, et al. An aqueous electrolyte polyionic large-format energy storage device using a thick format composite $NaTi_2(PO_4)_3$/activated carbon negative electrode. J Power Sources, 2014 [submited for publication].

[24] EnerSys. Hup solar one warranty and adjustment agreement; 2005 <http://proto.hupsolarone.com/wp-content/uploads/2012/01/IND262-SolarOne-07-051.pdf> [accessed January 2014].

[25] Bouzerdoum M, Mellit A, Massi Pavan A. A hybrid model (SARIMA–SVM) for short-term power forecasting of a small-scale grid-connected photovoltaic plant. Sol Energy 2013;98(C):226–35.